

## Development of a Numerical Model for Investigating the EDI+GPI Engine

Y. Huang<sup>1,2</sup> and G. Hong<sup>1</sup>

<sup>1</sup> School of Electrical, Mechanical and Mechatronic Systems  
University of Technology, Sydney (UTS), NSW, 2007, Australia

<sup>2</sup> School of Energy and Power Engineering  
Huazhong University of Science and Technology, Wuhan, Hubei, 430074, China

### Abstract

This paper reports the development of a CFD model for investigating the ethanol direct injection plus gasoline port injection (EDI+GPI) engine. The model was developed using the commercial CFD code ANSYS FLUENT as a solver. The computational domain was meshed based on the scanned geometry of the cylinder head. Realizable  $k-\epsilon$  turbulence model was used to simulate the in-cylinder flows. The Eulerian-Lagrangian approach was used to model the evolution of the fuel sprays. The dual-fuel combustion process was modelled by the Extended Coherent Flame Model (ECFM) in the partially premixed combustion concept. A five-dimensional presumed Probability Density Function (PDF) look-up table was used to model the dual-fuel turbulence-chemistry interactions. The model was verified by the good agreement between the numerical and experimental results of spray shapes in a constant volume chamber and cylinder pressure on the EDI+GPI research engine. Sample simulation results showed that the model was capable to simulate the spray combustion process of the EDI+GPI engine and meet the needs of the investigation.

### Introduction

Ethanol direct injection is a new technology to make the use of ethanol fuel in SI engines more effectively and efficiently by taking the ethanol fuel's merits and avoiding its drawbacks. Researchers have investigated the application of ethanol direct injection (DI) to gasoline port injection (PI) engines experimentally. Dual-injection concept for using ethanol on SI engines was firstly proposed by Cohn et al. [1]. They proposed that a small amount of ethanol was directly injected into the cylinder as an anti-knock agent, while gasoline was port injected. By doing so, the engine knock propensity could be reduced due to the higher octane number of ethanol fuel, and supplemented by the cooling effect enhanced by direct injection and ethanol's greater latent heat. This makes it possible to increase the compression ratio and consequently increase the thermal efficiency. Following this idea, research has been conducted to investigate it as reviewed as follows.

Ford tested the dual-injection concept for knock mitigation on the 'Ecoboost' engine, where E85 was directly injected into the cylinder and gasoline is port injected [2]. Zhu et al. [3] studied the combustion characteristics of three different dual-injection strategies on a single cylinder SI engine. The dual-injection strategies included the gasoline PI plus gasoline DI, gasoline PI plus E85 DI and E85 PI plus gasoline DI. Wu et al. [4] tested the dual-injection concept to use bio-fuels, where the gasoline was used via PI and ethanol or DMF was used via DI. The knock mitigation ability of dual-injection strategy were tested [5]. More recently, Zhuang and Hong [6] focused on investigating the leverage effect of EDI+GPI.

In contrast to the experimental investigations as reviewed above, few publications have been found about numerical investigation

to EDI. Kasseris et al. [7] used 3-D CFD modeling to investigate the effect of intake air temperature on the amount of charge cooling realized. The simulation results showed that effective cooling of ethanol fuel was achieved in high temperature conditions in a turbocharged engine. However the simulated evaporation rate of ethanol fuel in low temperature conditions (naturally aspirated engine) was much lower than gasoline's [8]. This may limit the cooling effect of ethanol fuel.

The experimental studies reviewed above have shown the advantages of EDI+GPI over the conventional single fuel injection system. However, the in-cylinder mixture formation and combustion mechanisms of this new engine system remain as a hard task for experimental investigations. On the other hand, CFD tools offer the ability to exploit the detailed and visualised information about the complicated flow inside the cylinder which usually can only be acquired in costly experiments. Therefore CFD simulations have been adopted to address this task. To simulate the mixture formation and combustion processes, the model should include the detailed geometry of the cylinder head, the dynamic mesh that represents the movements of the piston and valves, a set of numerical models for the in-cylinder flows, fuel sprays and combustion, appropriate initial and boundary conditions, and model validation. This paper reports a CFD approach to simulate the air/fuel mixing and combustion processes in an EDI+GPI engine that has been experimentally investigated [6].

### Geometry and Dynamic Mesh

The computational mesh was generated based on the engine equipped with EDI+GPI used in the experiments. Table 1 lists the engine specifications. The geometry of the cylinder head was scanned by a local company Qubic. The point spacing resolution of the scan is 0.2 to 0.4 mm. As shown in figure 1, the geometry includes the intake manifold with the throttle, the spark plug, the moving piston and the intake and exhaust valves.

Engine type	Single cylinder, air cooled, four-stroke, SOHC
Displacement	249.0 cc
Stroke × Bore	58.0 mm × 74.0 mm
Connecting rod	102.0 mm
Compression ratio	9.8:1
Valve timings	IVO: 22.20 CAD BTDC @0.25 mm lift IVC: 53.80 CAD ABDC @0.25 mm lift EVO: 54.60 CAD BBDC @0.25 mm lift EVC: 19.30 CAD ATDC @0.25 mm lift
Ethanol delivery system	Direct injection
Gasoline delivery system	Port injection

Table 1. Specifications of the engine to be modelled.

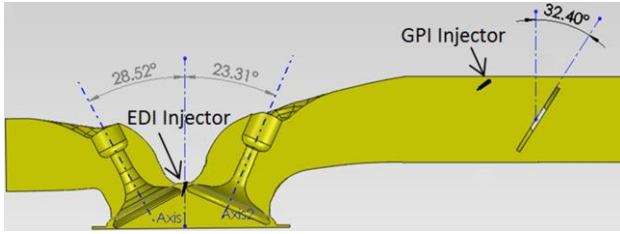


Figure 1. Cross-sectional view of the geometry of the cylinder head.

The geometry was pre-processed by the ANSYS DesignModeler. As shown in figure 2, the geometry was decomposed around the piston and valve volumes so that they could be meshed to different types of grid. The dynamic mesh was generated by the ANSYS Meshing. Three dynamic mesh schemes, namely smoothing, layering and remeshing, were used to tackle the challenge of moving boundaries of the piston and valves. As shown in figure 3, the mesh mainly consists of tetrahedral grids. However the regions with moving boundaries were meshed to hexahedral grids for mesh deforming. The general cell size for the mesh was 4.00 mm, while the cell size near the valve seat regions was refined to be 0.4 mm. The position of the piston was calculated as a function of the crank angle degree, the engine stroke and the length of the connection rod. The moving boundaries of the intake and exhaust valves were meshed based on the measured cam lift curves. To avoid extremely small gaps between the valve and the valve seat, it was defined that the intake and exhaust valves were open/closed when the valve lift was larger/smaller than 0.50 mm. As there was a minimum lift, the actual valve opening would allow too much flow into the chamber. To avoid this problem, the valve opening and closing angles were calculated using the trapezoidal method of numerical integration. The grids for the intake or exhaust manifolds were deactivated when the valve was closed in order to save the computation time. Three meshes with different grid densities were generated to test the mesh dependency. Strong grid dependency in terms of cylinder pressure has not been observed with the three meshes. Fewer nodes resulted in a poor quality mesh. Therefore, the mesh with the least nodes was adapted.



Figure 2. Geometry decomposition.



Figure 3. Computational mesh.

## Numerical Models

The numerical models were developed using ANSYS FLUENT. Realizable  $k-\epsilon$  turbulence model was used to simulate the in-cylinder flows. Standard Wall Functions were used for the near-wall treatment. Calculations with three time steps, 1.00, 0.50 and 0.25 crank angle degree (CAD), were performed. Time step larger than 0.25 CAD resulted in incomplete droplets. Incomplete droplets are that failed to be tracked by the code and disappeared in the computational domain. Therefore the time step

was set to 0.25 CAD. The time step was reduced during the transient periods when the valve was opening or closing and during the fuel injection to achieve a more stable and convergent calculation. As shown in table 2, the spray combustion model consists of eight sub-models, including the spray breakup, evaporation, distortion and drag, wall interaction, spark ignition, combustion and emission formation. These sub-models will be discussed in greater details in the following sections.

Droplet initialization	Rosin-Rammler Distribution Method
Breakup model	WAVE
Evaporation model	Convection/Diffusion Controlled
Drag model	Dynamic Drag model
Wall interaction	Wall jet
Spark model	Zimont model
Combustion model	ECFM partially premixed combustion
NO model	Extended Zeldovich mechanism

Table 2. Sub-models for dual-fuel spray combustion.

### Breakup Model

Droplet breakup is one of the most important processes in modelling the liquid fuel spray. However, modelling spray primary breakup is a difficult task because of the unsolvable uncertainty in the inner structure and fundamental mechanisms of liquid atomization. An approximate method to represent the complexity of initial atomization is to specify larger droplets or blobs similar to the injector nozzle diameter at the nozzle exit and model the secondary breakup using various droplet breakup models (blob injection concept). In this modelling, Rosin-Rammler Diameter Distribution Method was used to specify the initial droplet size at the nozzle exit. It is assumed that an exponential relationship exists between the droplet diameter  $d$  and the mass fraction  $Y_d$  of droplets with diameter greater than  $d$ :

$$Y_d = e^{-(d/\bar{d})^n} \quad (1)$$

where  $\bar{d}$  is the mean diameter,  $n$  is the spread number. For GPI spray droplets, the mean diameter was set as 300  $\mu\text{m}$ . For EDI spray droplets, the mean diameter was 110  $\mu\text{m}$ . The spread number is 3.5 for the two sprays. To achieve an accurate statistical representation for the particles, a large number of parcels should be introduced into the computational domain. Therefore 20 parcels of gasoline and ethanol per hole were released in each time step.

The droplets present different breakup mechanisms with the increase of relative velocity between the droplets and the ambient gas. Based on the breakup mechanism, secondary breakup can be classified into three regimes: bag breakup, stripping breakup and catastrophic breakup. A number of breakup models have been developed based on different breakup mechanisms. The Weber number is a reliable indicator for choosing a breakup model. In this modelling, although the initial velocity of the gasoline droplet was relatively slow at low pressure (0.25 MPa) GPI spray, the air velocity in the intake manifold could be as high as 200 m/s, as shown in figure 8. The Weber numbers for both GPI and EDI were greater than 100. Therefore WAVE breakup model was chosen. As an initially spherical droplet moves through the air, its shape is distorted significantly when the Weber number is large. This changes the droplet drag coefficient greatly. The Dynamic Drag model took account of the effect of droplet distortion.

### Evaporation Model

Fuel droplet's evaporation plays a crucial role in the mixture formation and combustion because the fuel droplets must

vaporize before they can burn. The Convection/Diffusion Controlled Model was used to simulate the ethanol and gasoline droplets evaporation. It incorporates both gradient diffusion and convection effects on the droplet evaporation process. The fuel properties, such as surface tension, enthalpy of vaporization and saturation vapour pressure etc., can significantly affect the spray breakup, evaporation and combustion processes. Therefore, it is critical to define the fuel properties correctly in the simulation. The properties of the ethanol fuel in the present study were provided in the Yaws Handbook [9]. Gasoline fuel contains various organic compounds ranging from C<sub>2</sub> to C<sub>14</sub>. The physical and chemical properties of iso-octane are similar to gasoline's and it is commonly used to represent gasoline fuel in experimental and numerical investigations. Particularly, saturation vapour pressure is an important factor indicating the liquid's volatility and it is the driving force for the droplet evaporation process incorporated in the Convection/Diffusion Controlled Model. It was found that the vapour pressure of gasoline was very different from that of iso-octane, as shown in figure 4. So the vapour pressure for gasoline was taken from the experimental data published in [10].

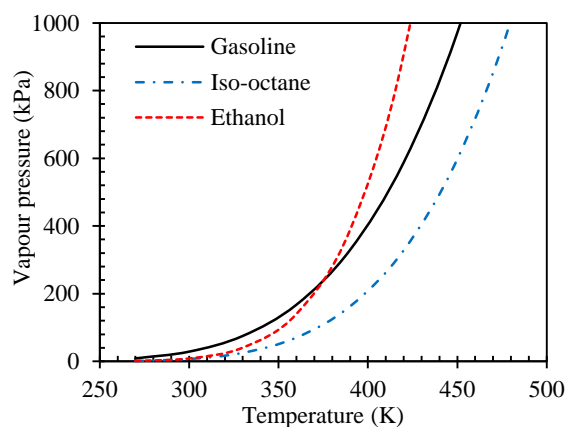


Figure 4. Variation of saturation vapour pressures with temperature for ethanol [9], iso-octane [9] and gasoline [10] fuels.

### Combustion Model

Spray combustion in SI engines is the partially premixed combustion which shows features of both non-premixed and premixed combustion. The fuel is injected into the combustion chamber in liquid form. The evaporation and diffusion processes occur prior to the combustion. By the time of combustion, part of the fuel has mixed with the oxidizer in molecular level but inhomogeneously, and evaporating and mixing processes are still going on. The partially premixed combustion model is usually a combination of premixed and non-premixed combustion models in which both the progress variable  $c$  and the mixture fraction  $Z$  are solved.

The ECFM combustion model has been adopted, which is applicable for internal combustion engines typically operated in the wrinkled flamelet range. The ECFM model strongly depends on the accuracy of the expression for the laminar flame speed. However an accurate analytical expression for burning velocity of premixed turbulent combustion is still unavailable. Instead the experimental data in [11] for ethanol and gasoline laminar flame speeds were used in this study. As shown in figure 5, ethanol fuel has higher flame speed than gasoline does over a wide range of equivalent ratio.

The combustion process is initiated in the Zimont model by releasing a specific amount of energy to the cells at the spark plug gap. The presumed PDF look-up table was used to model the turbulence-chemistry interactions. For single fuel GPI only combustion modelling, a three-dimensional PDF table was

generated to determine the temperature, density and species fraction in the turbulent flame. For dual-fuel EDI+GPI combustion modelling, a five-dimensional PDF table was generated to take into account the secondary fuel. The computational cost of implementing five-dimensional PDF table is much higher than three-dimensional one. In this study, the computation time was about 73 hours for EDI+GPI and 19 hours for GPI only on a 16-core Intel(R) Xeon(R) E5-2687W @ 3.1 GHz workstation.

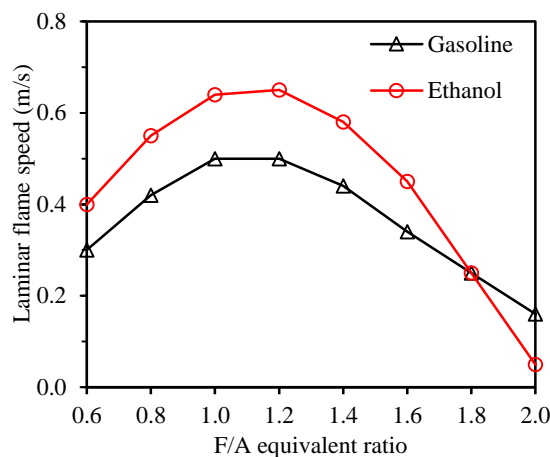


Figure 5. Laminar flame speeds of ethanol and gasoline fuels [11].

### Boundary and Initial Conditions

The boundary and initial conditions were set up to be the same as that in the experimental conditions. The engine speed was 4000 rpm, throttle was 36% open and the spark timing was 15 CAD BTDC. The average equivalent ratio was stoichiometric ratio for both EDI+GPI and GPI only operation conditions. For EDI+GPI, the ethanol ratio (by volume) was 46% which contains 8.54 mg gasoline and 8.00 mg ethanol. For GPI only, the mass of the gasoline injected was 13.40 mg with equivalent heating energy as that in EDI+GPI. The injection durations for the two injectors were calculated from the injection pressure and mass of the fuel injected. The wall temperature was set up based on the typical temperature distribution for SI engines operating at normal steady state conditions. The inlet and outlet pressure values were constant as the atmosphere pressure. The intake air temperature was set to be the room temperature of the engine laboratory. Initial conditions for the cylinder, intake and exhaust manifolds were set up according to the measured in-cylinder pressure and exhaust gas temperature.

### Model Verification

Firstly, the spray model was used to simulate the EDI spray process in a constant volume chamber. The injection pressure was 6.0 MPa, the ambient pressure was 1 bar and the ambient temperature was 350 K. This condition reproduced the cylinder conditions of early EDI injection at 300 CAD BTDC in engine experiments. The numerical results of the spray pattern and spray tip penetration were compared with the experimental ones. As shown in figure 6, the spray structure including its penetration length was well simulated by the fuel spray model.

The verified spray model was then incorporated into the engine model for simulating the mixture formation and combustion processes of GPI only and EDI+GPI. It simulated the process starting from GPI injection and ending at the exhaust top dead center. To verify the engine model, comparison was made between the in-cylinder pressure of the numerical and experimental values. As shown in figure 7, the numerical and experimental results of cylinder pressure agree well.

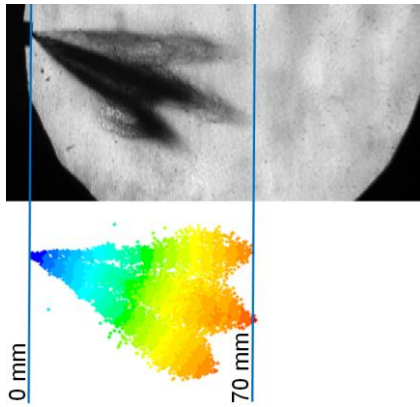


Figure 6. Comparison of the experimental and numerical EDI spray patterns at 1.5 ms after the start of injection.

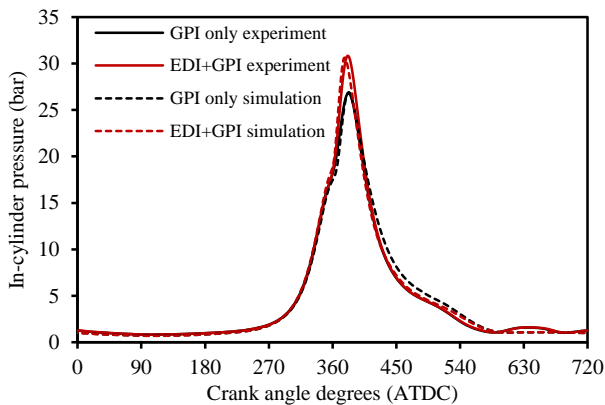


Figure 7. Comparison of measured and simulated in-cylinder pressure predicted for GPI only and EDI+GPI.

### Sample Simulation Results

Figure 8 shows the spatial distribution of the spray droplets and air flow velocity vectors on the engine symmetry plane at 15 CAD after the start of EDI. It shows that two horizontal swirls form near the cylinder wall during the intake stroke. These swirls should increase the heat and mass transfer between the fuel liquid droplets and the intake air, thus accelerates the fuel evaporation and enhance the mixing.

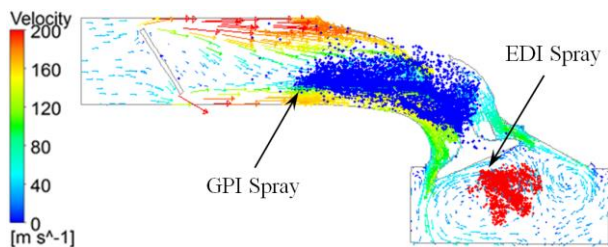


Figure 8. Spray droplet spatial distribution and air flow velocity vectors of EDI+GPI at 15 CAD after the start of EDI.

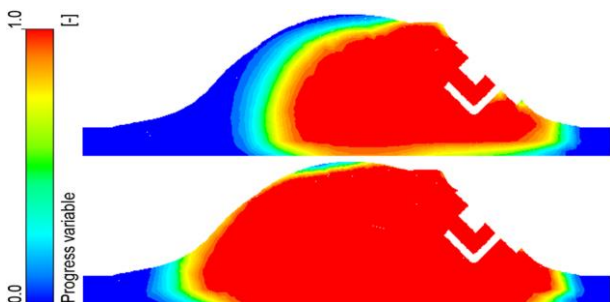


Figure 9. Propagation of the flame at 30 CAD after the spark timing of GPI only (top) and EDI+GPI (bottom).

In premixed combustion models, the progress variable  $c$  is introduced to indicate the state of the reactants, where  $c=0$  stands for fresh mixture and  $c=1$  stands for burnt mixture. Figure 9 shows the propagation of the flame on a vertical plane passing through the spark plug at 30 CAD after the spark timing. It can be seen that the flame in EDI+GPI mode propagates much faster than that in GPI only. This can be attributed to ethanol's faster laminar flame speed which is shown in figure 5.

### Conclusions

1. To investigate the in-cylinder mixture formation and combustion mechanisms in an EDI+GPI engine, a numerical model was developed. The model included the geometry of the cylinder head, a set of numerical models for the in-cylinder flows, dual-fuel sprays and combustion, and model validation.
2. The developed model was verified by good agreement between the numerical and experimental results of spray pattern and in-cylinder pressure.
3. Sample simulation results showed that the model was capable to simulate the air-fuel mixing and combustion processes of the EDI+GPI engine and meet the needs of the investigation.

### Acknowledgements

The scholarship provided by the China Scholarship Council (CSC) is gratefully appreciated.

### References

- [1] Cohn, D.R., Bromberg, L. & Heywood, J., Fuel Management System for Variable Ethanol Octane Enhancement of Gasoline Engines, *US Patent 2010175659*, 15 July, 2010.
- [2] Stein, R.A., House, C.J. & Leone, T.G., Optimal Use of E85 in a Turbocharged Direct Injection Engine, *SAE Int. J. Fuels Lubr.*, 2, 2009, 670-682.
- [3] Zhu, G., Hung, D. & Schock, H., Combustion characteristics of a single-cylinder spark ignition gasoline and ethanol dual-fuelled engine, *Proc. IMechE Part D: Automobile Engineering*, 224, 2010, 387-403.
- [4] Wu, X., Daniel, R., Tian, G., Xu, H., Huang, Z. & Richardson, D., Dual-injection: The flexible, bi-fuel concept for spark-ignition engines fuelled with various gasoline and biofuel blends, *Applied Energy*, 88, 2011, 2305-2314.
- [5] Daniel, R., Wang, C., Xu, H., Tian, G. & Richardson, D., Dual-Injection as a Knock Mitigation Strategy Using Pure Ethanol and Methanol, *SAE Int. J. Fuels Lubr.*, 5, 2012, 772-784.
- [6] Zhuang, Y. & Hong, G., Primary Investigation to Leveraging Effect of Using Ethanol Fuel on Reducing Gasoline Fuel Consumption, *Fuel*, 105, 2013, 425-431.
- [7] Kasseris, E. & Heywood, J. Charge Cooling Effects on Knock Limits in SI DI Engines Using Gasoline/Ethanol Blends: Part 1-Quantifying Charge Cooling, *SAE paper 2012-01-1275*, 2012.
- [8] Srivastava, S., Schock, H., Jaber, F. & Hung, D.L.S. Numerical Simulation of a Direct-Injection Spark-Ignition Engine with Different Fuels, *SAE paper 2009-01-0325*, 2009.
- [9] Yaws, C.L., *Yaws' Handbook of Thermodynamic and Physical Properties of Chemical Compounds*, Knovel, 2003.
- [10] Kar, K., Last, T., Haywood, C. & Raine, R., Measurement of Vapor Pressures and Enthalpies of Vaporization of Gasoline and Ethanol Blends and Their Effects on Mixture Preparation in an SI Engine, *SAE Int. J. Fuels Lubr.*, 1, 2008, 132-144.
- [11] Tian, G., Daniel, R., Li, H., Xu, H., Shuai, S. & Richards, P., Laminar Burning Velocities of 2,5-Dimethylfuran Compared with Ethanol and Gasoline, *Energy & Fuels*, 24, 2010, 3898-3905.